CHARACTERIZATION OF HYBRIDOMA ANTIBODIES TO IDENTIFY AUTOANTIGENS IN THE MOUSE MODEL OF SJŐGREN'S SYNDROME-LIKE DISEASE

By

MAURO ALEJANDRO TUDARES HERNÁNDEZ

A THESIS PRESENTED TO THE GRADUATE SCHOOL
OF THE UNIVERSITY OF FLORIDA IN PARTIAL FULFILLMENT
OF THE REQUIREMENTS FOR THE DEGREE OF
MASTER OF SCIENCE

UNIVERSITY OF FLORIDA

2009

To myself

ACKNOWLEDGEMENTS

I want to thank Dr. Ammon B. Peck for giving me the opportunity to carry out this project. I also want to thank members of my supervisory committee, Dr. Seunghee Cha and Dr. Shannon Wallet for giving me valuable guidance and advice regarding my research project. Marievic Bulosan, Janet Cornelius, and Dr. Coung Nguyen provided helpful technical recommendations. In addition, I thank my mom and family for providing support throughout the years.

TABLE OF CONTENTS

page

LIST OF TABLES

LIST OF FIGURES

Abstract of Thesis Presented to the Graduate School
of the University of Florida in Partial Fulfillment of the
Requirements for the Degree of Master of Science

CHARACTERIZATION OF HYBRIDOMA ANTIBODIES TO IDENTIFY AUTOANTIGENS IN THE MOUSE MODEL OF SJŐGREN'S SYNDROME-LIKE DISEASE

By

Mauro Alejandro Tudares Hernández

August 2009

Chair: Ammon B. Peck
Major: Medical Sciences

Sjögren's syndrome is a chronic autoimmune disease characterized by loss of secretion of tears and saliva from lachrymal and salivary glands respectively, lymphocytic infiltration of lachrymal and salivary glands, autoimmune attack against exocrine tissue and abnormal expression of cytokines. Several interacting factors may contribute to the onset of overt disease. One of the key events during the pathogenesis of the disease is the appearance of autoantibodies. They have a crucial role both as effectors and biomarkers of the disease.

B cells from draining lymph nodes of the of C57BL/6.NOD-Aec1Aec2 mice diagnosed with late-stage Sjögren's syndrome-like disease were fused with immortal murine myeloma cells in order to obtain antibody-secreting hybridomas that replicate the autoantibody response in the lymph nodes of this mouse model.

Supernatants from a set of hybridomas were screened to determine their reactivities against cellular antigens using Hep-2 cells and immunohistochemistry. Western blotting was used to test the reactivity of representative supernatants to cellular antigens according to molecular weight, leading to potentially more precise results identification of autoantigens by immunoprecipitation and gel sequencing analyses using GC-mass spectrometry.

Ninety-one proteins were identified representing several expected cellular autoantigens, including ribonuclear proteins, histones and structural proteins; however, definitive identification of any autoantigen among these ninety-one proteins will require additional studies. Nevertheless, these studies identified possible important proteins, constituting a novel opportunity to help elucidate the complex autoantibody responses that occur in the lymph nodes of the *C57BL/6.NOD-Aec1Aec2* mouse model of Sjögren's syndrome.

CHAPTER 1
INTRODUCTION

Definition of Sjögren's Syndrome

Sjögren's syndrome (SS) is a systemic disease characterized by a chronic autoimmune attack to various organs in the body, especially the exocrine tissues of the lacrimal and salivary glands, causing abnormalities in the quantity and quality of tears and saliva, respectively, leading to numerous health problems. Additional target organs that might be affected include the thyroid gland, kidneys, liver, lungs, skin, peripheral nerves, joints, and muscles causing numerous conditions that diminish the quality of life. Some patients may also develop life-threatening diseases such as malignant lymphoma. Key features of the autoimmune attack consist of lymphocytic infiltration of target tissues, increased secretion of cytokines by T cells, and increased production of autoantibodies by B cells.

Primary Sjögren's Syndrome.

Primary Sjögren's syndrome (pSS) is characterized by a decrease in the function of exocrine glands without clinical or laboratory evidence of any other autoimmune disease. Dysfunction of the lacrimal and salivary glands is early and progressive, as seen in mouse model of the disease (Nguyen et al., 2007). Extraglandular tissues may be affected as well in pSS.

Secondary Sjögren's Syndrome.

Secondary Sjögren's syndrome (sSS) occurs in people who have been diagnosed previously with other autoimmune connective tissue diseases. The two entities most commonly associated with secondary Sjögren's syndrome are rheumatoid arthritis (RA) and systemic lupus erythematosus (SLE) (Fox, R., 2005). In contrast, the non-obese diabetic (NOD) mouse develops type 1 diabetes (T1D) and SS. T1D is an autoimmune disease characterized by a T cell mediated destruction of pancreatic β-cells. Nevertheless, SS in the NOD mouse is classified as sSS. In sSS

the degree of damage to the lacrimal and salivary glands can be less severe than in pSS as the disease in the two glands can occur separately (Nguyen et al., 2007)

Pathogenesis

Development and onset of Sjögren's syndrome is the result of a combination of genetic, environmental, and immunological factors not yet completely deciphered (Nguyen, Singson et al., 2006). Environmental factors have minimum impact on animal models of the disease, thus, emphasis on genetic and immunological factors in mice will be discussed here.

The similar clinical features between human and mice SS provides a practical mechanism to extrapolate findings from mice studies into the human context of the disease. Up to now, genetic recombination studies in the NOD mice model of the disease have provided evidence as to how genetic predisposition may influence the development and onset of Sjögren's syndrome. Initially, these studies aimed at analyzing the potential role of genes of the MHC, finding predisposition associated with markers from this genomic region (Fei et al., 1991)

Further studies focused on the potential role of insulin dependent diabetes susceptibility genes in glandular exocrine dysfunction and development of autoimmunity, based on the assumption that if these genes have an influence on the development and onset of diabetes in the NOD mice, then it would be possible that the same was true for SS (Brayer et al., 2000). There are more than 21 chromosomal regions thus far known to be positive contributors to the development of diabetes in the NOD mice (Brayer et al., 2000). Each chromosomal region is a genetic interval of precise distance and is called diabetes susceptibility loci or *idd*. To assess the potential role of each one of these twenty-one single *idd* over the development and onset of SS, they were individually replaced from the NOD mice and inserted in the disease free C57BL/6 mice using genetic backcross techniques. Opposite to what it was expected, results from these studies showed no development of autoimmune exocrinopathy in the C57BL/6 mice when each *idd* loci

was individually replaced, leading to the conclusion that single genetic *idd* segments, with proved positive influence over the development and onset of diabetes, do not have a role in the pathogenesis of Sjögren-like disease when recombined individually in the C57BL/6 mice (Brayer et al., 2000).

Moving past the effect of single *idd* alleles over the development of Sjögren-like disease in the C57BL/6 mice, studies went on to evaluate the potential role of a combination of *idd* segments over the development of SjS-like disease. Again, previous diabetes studies lead now to this assumption (Hill, N.J., et al, 2000). Not surprisingly, it was found that *idd5* alleles from chromosome 1 and *idd3* alleles from chromosome 3 of NOD mice together contribute additively to the development of autoimmune exocrinopathy when replaced in the C57BL/6 mice (Brayer et al., 2000).The development of SjS-like autoimmune response in these studies was evidenced by the presence of histological sialoadenitis lesions, appearance of serological markers of the disease such as antinuclear and cytoplasmic antibodies, and abnormal results from physiological tests such as measurement of saliva flow rates, protein concentration, amylase activity, and cysteine protease activity (Brayer et al., 2000). Later on, *idd5* genetic region on chromosome 1 was designated *Aec2*, and *idd3* genetic region on chromosome 3 was designated *Aec1* (Aec = autoimmune exocrinopathy) leading to the generation of the C57BL/6.NOD-Aec1Aec2 murine model for primary Sjögren's syndrome which is homozygous for both the *idd3* and *idd5* genetic intervals and does not exhibit many of the dysfunctional immune features of the NOD mice (Cha et al., 2002).

Both *Aec1* and *Aec2* loci have a different gene pool, length, and role in the pathogenesis of SjS-like disease (Nguyen, Singson et al., 2006). The length and limits of A*ec1* and *Aec2* are different and were identified using microsatellite markers (Nguyen, Singson et al., 2006). *Aec1* is

a 48.5 cM (centimorgan) region (Nguyen, Singson et al., 2006) that contain four diabetes susceptibility alleles: *Idd3, Idd10, Idd17*, and *Idd18*, as well as the gene for IL-2. A 0.15cM region from chromosome 3 has been implicated in the development of experimental autoimmune encephalomyelitis and diabetes (Encinas et al., 1999 and Sundvall et al., 1995). *Aec1* is associated with the immune and clinical phase of the disease in the mice model.

Aec2 is associated with the initial, preclinical or non-immune phase of the disease in which autoimmunity events are not yet detectable, (Nguyen et al., 2007). *Aec2* is a 68.4 cM genetic region comprising the gene locus for bcl-2, and genetic loci for caspase-8 and cytotoxic T-lymphocyte-associated antigen-4 (CTL-4) (Brayer et al., 2000 and Nguyen et al., 2006). CTLA-4 is a 33 kDa molecule that negatively regulates T-cell activation. It is also called CD152 and it has been shown to play an important role in T-cell homeostasis and autoimmune diseases, since mice deficient in CTLA-4 develop lymphoproliferative disorders and die early in life due to tissue destruction of multiple organs (Lundholm et al., 2006) . Likewise, NOD activated T-cells show anomalous expression of CTLA-4. In this scenario, cytokines such as IL-2, can contribute to up-regulated transcription of CTLA-4, especially upon T-cell activation through the CD3 complex in vitro; rendering CTLA-4 readily available on the cell surface (Lundholm et al., 2006).

It has been mentioned before about the synergistic role of *Aec1* and *Aec2* genetic regions on the development of Sjögren's syndrome. Few studies so far have tried to understand the molecular mechanisms of such a genetic symbiosis in the C57BL/6.NOD-*Aec1Aec2* mice. However, some other studies have been aimed at understanding more precisely how different type-1 diabetes susceptibility genes located in distinct chromosomal regions may interplay at early phases during type-1 diabetes initiation in the NOD mice. For instance, it has been shown

that *Ctex* and *Idd3* down-regulate *Ctla-4* in the NOD mice (Lundholm et al., 2006). *Ctex* is a 21 cM, telomeric novel locus identified by interval mapping methodology that positively contributes, along with *Idd3*, to the defective expression of *Ctla-4* (Lundholm et al., 2006). In this context, the molecular role of inadequately expressed *Ctla-4* in susceptibility and initiation of diabetes is not well understood to date, but blockage of the protein using antibodies targeted against the full-length structure of it increases the appearance of overt diabetes in the NOD mice probably because of activation of cytotoxic T-cells (Lühder et al., 1998 and Luhder et al., 2000). Likewise, the linkage between *Ctla-4* down regulation and development of lymphoproliferative disorders and autoimmunity represents a promising research topic that would help to better understand the primary molecular processes that lead to the development of these conditions.

Interestingly, *Idd5* contains the *Bcl-2* locus as mentioned above. This fact deserves special consideration. *Bcl-2* is an oncogene that promotes cell survival and proliferation (Petros et al., 2004). It is part of the Bcl-2 family of genes that includes both cell survival (*Bcl-2, Bcl-XL, Mcl-1, Ced-9, A1, Bfl-1*) and cell death (*Bax, Bak , Diva, Bcl-Xs, Bik, Bim, Bad, Bid, Egl-1)* genes important for maintenance of cell homeostasis (Kaufmann et al., 2004). Cancers, for instance, B-cell lymphomas, arise when cell conditions favor gene expression of cell survival genes over cell death genes; stimulating proliferation and inhibiting apoptosis. Apoptosis is important to maintain a lymphocyte population within the normal values. During infection states, active production of lymphocytes occurs and the number of these cells increases rapidly as a response to the presence of foreign pathogens. Accordingly, *Bcl-2* expression increases to sustain and extend lymphocyte presence. *Bcl-2* inhibits programmed cell death by binding to the mitochondrial outer membrane and inhibiting the release of cytochrome-c into the cytoplasm. Antigen-receptor signaling plays an important role in the maintenance and survival of

lymphocytes as well. No evidence so far links Bcl-2 over expression as an explanatory factor of B-cell lymphocyte proliferation in SS. However, it would be important to address whether or not the presence of *bcl-2* locus in the *Aec-2* chromosomal region is an important co-regulatory factor stimulating lymphocyte proliferation is SS.

The *Aec1* locus has been redefined more precisely to a region of just 20cM by generation of a recombinant inbred line of C57BL/6.NOD-*Aec1R1Aec2* that shows a crossover region within chromosome 3 (Nguyen et al., 2006). Under these genetic circumstances both male and females showed similar autoimmune phenotype of the parental C57BL/6.NOD-*Aec1Aec2*, but females failed to develop lymphocytic infiltrates in the lachrymal glands and full blown SS disease, perhaps indicating that key genes associated with SS phenotypic gender differences are located within the removed genetic segment of approximately 30cM. Close location of the *IL-2* gene to the area of the cross-over region in chromosome 3, might help to further understand the pathogenesis of SS. Among other functions IL-2 is known for inducing secretion of antibodies by B lymphocytes and generation of Treg cells. In SS, increase production of autoantibodies occurs, especially in later phases of the disease. A direct role of IL-2 in triggering autoantibody production in SS remains speculative but needs to be studied. *IL-7 gen* is also located in the crossover region. IL-7 is a cytokine involved in B-cell proliferation and maturation as well. Expression of IL-7 could be implicated in the pathogenesis of SS via the inhibition of apoptosis of B cells by an indirect mechanism. Carbonic anhydrase and retroviruses genes are also found in the redefined *Aec1R1* locus. However, their possible role in the pathogenesis of SS is logical but has not been studied yet.

Recent studies have tried to understand more precisely the *Aec2* region of chromosome 1 as well, and its influence on the development of pathogenesis of SS. To do so, recombinant

inbred lines of the C57BL/6.NOD-*Aec1Aec2* mouse have been generated in order to screen for appearance of crossover segments within this loci (Nguyen et al., 2008). One new line, C57BL/6.NOD-*Aec1Aec2R (n)*, is homozygous for a crossover region in the *Aec2* loci and is the result of inbreeding the C57BL/6.NOD-*Aec1Aec2* mouse with the C57BL/6J mouse. Such an approach provided new clues about the presence of genes located within this region, which are valuable to study their potential involvement in the pathogenesis of the disease. It was found that the QTL-*Ath1* domain within this new delineated crossover *Aec2* region contains genes of particular importance such as *Ox40L* and *Tnfsf6*. FasL is the product of *Tnfsf6* and is up-regulated in the early phases of SS in mice, perhaps in association with increased glandular cell apoptosis typical of this phase. *Ox40L (Tnfsf4)* encodes OX40L, an important protein found to be involved in preventing the maturation of $T_{reg}1$ cells, and in the regulation of fatty acids metabolism.

In summary on the importance of genetic regulation in the development and onset of Sjögren's syndrome; in the absence of strong evidence regarding the association of class II MHC with SS, studies shifted direction to focus on the potential role of *idd* regions as key factors contributing to the pathogenesis of SS. Evidence showed that NOD derived *Aec1* and *Aec2* chromosomal regions both play an important role during initiation and progression of the disease, as confirmed by studies done in the C57BL/6.NOD-Aec1Aec2 murine model of pSS. Moreover, the functional relationship between these two chromosomal intervals is additive and synergistic, suggesting that the regulation of the expression of genes within *Idd3* or *Idd5* loci is not confined within each region separately but, instead, genes within *Idd5* loci have genetic regulation elements located in the *idd3* chromosomal interval. For instance, IL-2 (*IL-2* is located *close to Idd3*) signaling is associated with mobilization of CTLA-4 (*CTLA-4* is located in *Idd5*)

from intracellular vesicles to the cellular membrane in CD3 activated-T cells. Contradictorily, low levels of CTLA-4 are required for proper T-cell activation, suggesting that CTLA-4 expression might be under different transcriptional control in naïve and activated T-cells. In the other hand, regulation of *Idd3* genes of importance for the development of Sjögren's syndrome has not been yet thoroughly approached in the primary murine model of the disease. However, notable advance has been made identifying potential candidate genes for development and onset of SS in the mouse model by creating crossover regions of both *Idd3* and *Idd5*. In this context, the genetic interaction of *Bcl-2* with elements of the *idd3* or other locus, as a contributory factor in pathogenesis of SS remains to be elucidated.

Phases in the Pathogenesis of Sjögren's Syndrome-like Disease.

Three phases have been described in the C57BL/6.NOD-*Aec1Aec2* mouse model of the disease (Cuong et al., 2006). The first phase is non-immune and goes until about eight weeks of age. Important events include abnormal development of glands with altered expression of acinar antigens, and activation of apoptosis markers such as caspase-3 and caspase-11. The presence of elevated levels of INFy may reflect early involvement of viruses in this phase of the pathogenesis of the disease. Second phase starts around eight to nine weeks. Main ongoing events are a consequence of alterations that occurred in the previous phase. Acinar cell apoptosis causes activation of an intense autoimmune response leading to leukocyte infiltration of target glands. Exposure of cellular antigens due to intracellular redistribution and apoptosis triggers the synthesis of autoantibodies that attack mainly nuclear antigens. Other autoantibodies are synthesized including the anti-M3R autoantibody. During the third phase starting at about 16 weeks, loss of secretory function occurs. However, decreased saliva and tear flow can be observed as soon as 12 weeks of age in the C57BL/6.NOD-*Aec1Aec2* mouse.

Role of Humoral Immunity in the Pathogenesis of Sjögren's Syndrome

Hypergammaglobulinemia and presence of serum autoantibodies are key clinical findings in patients with SS. Their appearance is dependent upon the onset of autoimmunity, and also they mediate much of the inflammatory process that leads to eventual dysfunction of salivary and lachrymal glands. Lately, much importance has been given to study the presence of autoantibodies reactive with the muscarinic receptors on acinar tissues of the salivary and lachrymal glands. In support of this concept, it was showed that congenic NOD B cell knockout mice (NOD.Igμ^{null}) develops exocrine gland lesions with small T cell lymphocytic infiltrates but do not show lachrymal or salivary dysfunction or high glucose levels. The absence of insulitis, diabetes, and exocrinopathy in the NOD.Igμ^{null} mice led to think that B lymphocytes play a key role in the onset of the pancreatic and glandular autoimmune attack.

In addition, the composition of the lymphocytic infiltrates in salivary glands is mostly at expense of B lymphocytes in autoimmune and clinical phases of the disease. These B cells are highly reactive and are responsible for continuous secretion of auto-antibodies and for the development of hypergammaglobulinemia (Cuong et al., 2006).

All taken together suggests that in Sjögren's syndrome like disease, B cells have a protagonist participation in the pathogenesis of the disease by infiltration of target organs, secretion of auto-antibodies, and in fewer cases, transformation of chronically stimulated B lymphocytes into lymphomas (Cuong C. et al, 2006). Of course, B cells do not act alone. As in all autoimmune disease, participation and activation of T cells is required (Bennett JC, 2008)

Role of autoantibodies in the pathogenesis of Sjögren's syndrome

Anti-Ro/SSA and Anti-LA/SSB Autoantibodies

Presence of serum anti-Ro(SSA) and anti-La(SSB) autoantibodies is part of the international classification criteria for Sjögren's syndrome in human patients (Vitali et al., 2002). Evidence of

serum levels of anti-Ro (SSA) and anti-La (SSB) in SS patients are clinically associated with early manifestation of signs and symptoms, longer disease progression, and occurrence of parotid gland enlargement. Likewise, presence of these autoantibodies correlates histologically with more dramatic lymphocytic infiltration of minor salivary glands (Mavragani et al., 2000) Although Ro (SSA) and La (SSB) are well known ribonuclear RNA-binding proteins and their physiological function has been studied extensively , the role of anti-Ro (SSA) and anti-La (SSB) autoantibodies in the pathogenesis of SS through recognition of their target antigens is not well understood yet (Tengnér et al., 1998) . So far, two Ro/SSA subunits have been identified: Ro 60 kD and Ro 52 kD. They can be both localized in the nucleus and cytoplasm depending on conditions of cell stress and homeostasis. Such a dynamic localization makes it harder to describe fluorescent patterns that can be universally accepted. While it is known that Ro 60 kD binds to cytoplasmic RNA, the intracellular interactions of Ro-52 are not clear yet and some argue that is not a Ro protein (Boire et al., 1995).

La (SSB) a 48 kD localized both in the nucleus and cytoplasm (de Wilde et al., 1996). It has binding capacity especially to the poly-U tail of RNA polymerase III transcripts (Gottlieb et al.,1989) and can depict a cytoplasmic patter of staining specially when studied in conjunctival epithelium (Yannopoulos et al., 1992). It is not known yet why both Ro (SSA) and La (SSB) are among the cellular targets of the autoimmune attack in SS, but cells secreting autoantibodies against Ro (SSA) and La (SSB) antigens have been locally identified to be in the affected salivary glands. In addition, anti-Ro (SSA) autoantibodies have been found on skin cells of patients with SLE (Golan et al., 1992). Thus, in the context of autoimmune exocrinopathy, anti-Ro (SSA) and anti-La (SSB) autoantibodies are thought to have a dual role both as markers of

the disease and mediators of the pathogenic events that lead to overt disease (Nguyen et al., 2007).

Anti- M3R Receptor Autoantibodies

The M3R receptor is a cell surface protein localized in exocrine and non-exocrine tissues across the body. It is responsible for the transmission of neurological signaling messages from the extracellular to the intracellular space, acting as a mediator during the secretion mechanism of salivary and lachrymal glands.

A functional M3R receptor is required for normal saliva and tear secretion. Auto-antibodies to the M3R receptor block post-ganglionic parasympathetic neurons innervating salivary and lachrymal glands by impeding transmission of acetylcholine to acinar and ductal cells, thus mediating glandular dysfunction and causing appearance of clinical disease (Yamamoto et al., 1996; Watermam et al., 2000).

In humans, anti-M3R antibodies have been found not only in pSS cases, but also in sSS associated with rheumatoid arthritis context (Watermam et al., 2000). This study found presence of anti-M3R antibodies in 5 out of 9 patients (55%) diagnosed with pSS, and 6 out of 6 patients (100%) diagnosed with sSS. Indirect evidence of anti-M3R antibodies existence was based on the results of experiments showing the inhibitory effect of patient's sera (n=11) on bladder smooth muscle contraction after in vitro stimulation of the M3R receptor with carbachol. Subsequently, IgG fraction was purified from sera samples. Purified IgG fraction produced inhibited bladder smooth muscle carbachol-evoked responses as well, consistent with results for sera alone. However, assuming no diagnostic errors at the time of enrollment and no experimental flaws; it cannot be concluded from this study that autoimmunity against M3R receptor is universally present across the study sample suffering from the disease, since sera from 44% of patients with pSS did not elicit significant inhibition of smooth muscle contraction.

Another finding that supports the participation of anti-M3R autoantibodies in the pathogenesis of SS is the persistence of normal secretory levels of tears and saliva in NOD.Igμ^{null} mice, a congenic strain lacking functional B lymphocytes (Robinson et al., 1998). The structural role of the anti-M3R autoantibodies is perhaps to bind directly to the M3R receptor. In this context, synthesis of anti-M3R autoantibodies and their interaction with the M3R receptor in pathogenesis of SS was demonstrated *in vitro* by initial incubation of mouse parotid gland membrane preparations with the muscarinic receptor agonist [^{3}H] quinuclidinyl benzilate ([^{3}H] QNB), and subsequent failure of the SS human IgG to immunoprecipitate the M3R receptor-[H^3] QNB complex; suggesting competition between SS human IgG and [H^3] QNB for the same binding site at the M3R receptor. Additionally, this experiment supports previous studies evidencing cross-reactivity between mice M3R and human IgG, and rules out any functional or structural dysfunction of the M3R receptor in SS, although hypothetically, its density may be diminished after chronic stimulation by anti-M3R receptor autoantibodies.

Desensitization of the M3R receptor is associated with chronic presence in sera of circulating auto-antibodies against the membrane protein, as assessed by studies evaluating carbachol-evoked responses on smooth muscle strips isolated from NOD mice during the third phase of the disease (Cha et al., 2006). In this study, anti-M3R autoantibodies initially improved cholinergic-like M3R responses during a short period of time. However, receptor's responses to agonist molecules diminished after prolonged stimulation by anti-M3R auto-antibodies. Desensitization of the M3R receptor is a consequence of continuous binding by anti-M3R antibodies, leading to an increased threshold level to cholinergic stimulation and decreased exocrine function of salivary and lachrymal glands due to reduced intracellular calcium concentration. It is still unknown whether or not binding of anti-M3R autoantibodies to the receptor elicits either

conformational changes or alters the expression of this membrane protein of the parasympathetic nervous system with consequent decrease of its density.

Antibodies that inhibit M3R receptor have been reported not only in patients with SS but also in patients suffering from scleroderma (Cavill et al., 2003); which is a chronic disease characterized by thickening of the skin along with vasculopathy and progressive fibrosis of multiple organs including lungs, kidneys, and gastrointestinal tract (Varga , 2008). Although participation of the Fc fraction cannot be discarded as a mediator of autonomic contractile dysfunction in vivo; studies aimed at exploring the inhibitory mechanisms of autoantibodies found that both the Fab (monovalent) and $F(ab')_2$ (divalent) fraction of patients' IgG functional autoantibodies are responsible for producing inhibition of smooth muscle contraction on functional assays (Cavill et al., 2003). On the contrary, non-SS patient's IgG did not elicit the same inhibitory effect. However, purified IgG from healthy individuals (n=4) was able to neutralize functional anti-M3R autoantibodies, but the mechanism involved, how this mechanism may differ from the one used by intravenous immunoglobulin (IVIG) antibodies, and in what circumstances it is activated are enigmas, have not been answered yet. IVIG is a purified pool of immunoglobulins that neutralizes autoantibodies' inhibition of smooth muscle contraction in a concentration dependent manner (Cavill et al., 2003); therefore it has been used to treat dysautonomia in SS (Dupond et al., 1999)

In summary, then, autoantibodies play a major role in the pathogenesis of SS, a concept strongly supported by multiple studies carried out in mice models of SS. As a result, identifying the nature and reactivity of autoantibodies is an important endeavor in understanding SS. In the following studies, I have initiated an approach that is designed to identify tissue-specific autoantigens by defining the reactivity of autoantibodies in a global analysis using hybridoma

supernatants generated from fusions of B lymphocytes isolated from the draining lymph nodes of diseased C57BL/6.NOD-*Aec1Aec2* mice. The overall question is whether or not such an approach is feasible. To address this question, I established 2 specific aims: a) to carry out a general characterization of supernatants reactivity using immunofluorescence and western blot analysis, b) to initiate a more precise identification of antibodies by carrying out immunoprecipitation and band sequencing analysis.

CHAPTER 2
MATERIALS AND METHODS

Animals

Male C57BL/6.NOD-*Aec1Aec2* mice were maintained under specific pathogen-free conditions in the Department of Animal Care Services at the University of Florida, Gainesville, Florida. The animals were provided food and water *ad libitum*. Twenty mice were euthanized at 20 weeks of age and their tissues harvested.

Indirect Immunohistochemistry

Hep-2 cells were grown in DMEM (with 10% FBS + antibiotic) at 37 ^{o}C until they reached 80-90 % confluency. Subsequently, they were trypsinized and counted. Four thousand cells per well were seeded in 8-well chamber slides and let grow overnight or until confluency reached 70-80%. At this time, cells were washed twice with ice-cold PBS and fixed with 100% methanol for 30 minutes. After two additional washes, 5 minute each with ice-cold PBS, 200 hundred µL of undiluted primary antibody (hybridoma supernatant) was layered over the cells and incubated for 1 hour at 4 ^{o}C. Simultaneously, supernatants were diluted at 1/50 and 1/100 in PBS, layered over the cells and incubated for the same amount of time at 4 ^{o}C, too. After two more washes with ice-cold PBS, cells were covered with Alexa Fluor 594 goat anti-mouse IgG (H+L) diluted 1/50 and incubated for 1 hour at 4 ^{o}C. After two additional washes, cellular fluorescence was visualized by fluorescence microscopy at 100x magnification.

Western Blotting

Hep-2 cells were grown in DMEM (with 10% FBS + antibiotic) at 37 ^{o}C until they reached 80-90 % confluency. Cells were washed twice with PBS, 2 ml of lysis buffer added (10mM Tris-HCL, 0.4 M NaCl, 1 mM EDTA, 1% Triton X-100 (vol/vol); pH 7.5) supplemented with 20 µL Protease inhibitor Cocktail Set I (Calbiochem, cat. # 539131), and scraped into a 1.5

microcentrifuge tube. Then, cells were vortexed for 3 minutes, incubated for 20 minutes on ice, vortexed again for 3 minutes, and centrifuged at 14.000 rpm at 4 ^{o}C for 20 minutes. Supernatant was collected and protein concentration determined.

Approximately 40 micrograms (~40 µL) of whole cell protein lysate was denatured by boiling it in 4X SDS buffer and size-separated using a 4-15% Tris-HCL gel electrophoresis gel (Bio-Rad, Hercules, Ca. Cat. # 161-1104) prior to transfer to PVDF membrane. Membrane was blocked overnight at 4 in blocking buffer (5% nonfat dry milk in TBS) with shaking. Next day, supernatants were diluted 1:10 in PBS and incubated separately with a piece of membrane at 4 ^{o}C with shaking. After overnight incubation, each piece of membrane was incubated with Goat Anti-Mouse IgM+IgG+IgA (H+L) (SouthernBiotech, Birmingham, Alabama; USA) diluted 1:800 at 4 ^{o}C with shaking for 1 hour. After three 15-minute washings with TBS, membrane was exposed to substrate for 1, 30 and 60 seconds and developed.

Immunoprecipitation

Hep-2 cells were grown in DMEM (with 10% FBS + antibiotic) at 37 ^{o}C until they were actively growing and reached 80-90 % confluency. Cells were trypsinized, counted, pelleted, and washed twice with PBS. Nuclear and cytoplasmic lysate was separated using the PARIS^{TM} Kit (Applied Biosystems, Texas; USA). After removing the PBS wash, pellet was resuspended in 500µL of ice-cold Cell Fractionation Buffer included in the kit. Following incubation on ice for 10 minutes, the suspension was centrifuged 5 minutes at 4 ^{o}C and 1000 rpm. The Supernatant (cytoplasmic fraction) was collected and 500 µL of Cell Disruption Buffer added to the pellet followed by vigorous vortexing to lyse the nucleus. Protein concentration was determined in both cytoplasmic and nuclear fractions.

Prior to the immunoprecipitation, 30 µL of protein-G agarose (Upstate, Lake Placid; NY. Cat # 16-266) was mixed overnight with 0.5 ml ice-cold PBS and 100 µL of supernatant or mouse

serum at 4 ^{o}C with end over end shaking. Next day, following centrifugation for 30 seconds at 13000 rpm, supernatant was collected and saved. Antibody-conjugated beads in the bottom of the microcentrifuge tube were washed twice with ice-cold PBS and mixed with 10 µL of 10% BSA plus 100 µL of either cytoplasmic or nuclear Hep-2 cells fractions for overnight incubation at 4 ^{o}C with end over end shaking. Next day, suspension was centrifuged 30 seconds at 13000 rpm, supernatant saved and pellet washed three times. Final pellet (~30 µL) was mixed with an aliquot of SDS (gel 1) or 50 µL of SDS and 50 µL of PBS (gel 2), boiled for 5minutes and analyzed by one-dimensional gel electrophoresis using a 4-15% Tris-HCL gel (Bio-Rad, Hercules, Ca. Cat. # 161-1104). Gel was stained overnight with Coomassie blue staining solution and de-stained with a de-staining solution (5% methanol, 10% glacial acetic acid).

Protein Band Identification Using Mass Spectrometry

To identify proteins isolated by immunoprecipitation, a set of gel bands selected using molecular weight estimates were sent to the ICBR Protein Core Facility.

CHAPTER 3
RESULTS

Immunohistochemistry

Forty supernatants obtained from the ICBR Hybridoma Core were analyzed. None of these supernatants were derived from cloned hybridomas, but all had been tested for reactivity on the Hep-2 cell line. As expected, all samples were positive for immunofluorescent staining of Hep-2 cells. Staining patterns of the 40 supernatants on Hep-2 cells were defined by six general patterns, and grouped: speckled (nuclear), nuclear membrane (nuclear rim), nuclear membrane line, nucleolar, cytoplasm (cytoskeletal), and cytoplasmic dot. Speckled pattern was observed in fifteen samples (37%), nuclear membrane (nuclear rim) pattern was observed in seven samples (17%), nuclear membrane line pattern was observed in five samples (13%), nucleolar pattern was observed in one sample (3%), cytoplasm (cytoskeletal) pattern was observed in eleven samples (27%), and cytoplasmic dot pattern was observed in one sample (3%). These six staining patterns are presented in Figures 3-1 and 3-2. For further analysis, a prototype supernatant was chosen as a representative for each pattern. Supernatant 2E6 was chosen as the prototype sample for speckled pattern, 1G7 for nuclear membrane, 5A9 for nuclear membrane line, 5A10 for nucleolar, 4F12 for cytoplasm, and 5C1as cytoplasmic dot pattern (Figure 3-3).

Nuclear Speckled pattern as seen in clone 2E6 (Figure 3-3, C): Fine and diffuse speckling is seen in the nucleus leaving almost no space for black, dark dots. Mitotic cells are not clearly visible in the frame possibly because of the strong staining of the cells, which is compatible with a La (SSB) pattern. The nucleoplasm is almost entirely stained and there are a few fluorescent dots visible in most of the nuclei of the cells and in the cytoplasm as well. This pattern of staining suggests that ribonuclear proteins such as Ro (SS/A), La (SS/B), or both might be the target antigens.

Nuclear membrane line as seen in clone 5A9 (Figure 3-3, D): There are one or two bands of intense staining surrounding the nucleus but it does not encircle it completely. The staining pattern of the nucleus is very diffuse and fluorescent dots are not visible. Target antigens might be part of the Golgi apparatus.

Cytoplasmic dot as seen in clone 5C1 (Figure 3-3, E): Numerous, small but very intense dots are seen exclusively in the cytoplasm of the cells. However, some cells show a complete nuclear membrane ring and a single fluorescent dot within this nuclear peripheral structure. Interestingly, the cluster of cytoplasmic dots are seen very closely associated with the nuclear structure, thus it might be hypothesized that these numerous cytoplasmic dots are nuclear projections coming from the nucleus. Truly depiction of cytoplasmic dots could be explained by the reaction of the assay against lysosomes. In the other hand, as mentioned before, nuclear pore antigens could also produce this pattern.

Nucleolar staining as seen exclusively in clone 5A10 (Figure 3-3, F): Bright fluorescent dots are seen associated with the nucleoplasm of the cell. The nucleus is covered with coarse-like speckles which is consistent with the idea that nucleolar patterns are usually associated with nuclear patterns. Target antigens might include Scl 70 protein, and other nucleolar proteins such as PM-1 and PL-6.

Cytoplasmic (cytoskeletal) staining as seen in clone 4F12 (Figure 3-3, G): Cytoplasm is uniformly stained and well delimited with respect of the surrounding area. Bright fluorescence intensity is seen in the cytoplasmic. Target cellular antigens representing this pattern might be actin, tubulin, and/or vimentin.

Nuclear membrane (nuclear rim) staining as seen with clone 1G7 (Figure 3-3, H): A complete halo of fluorescence is seen around the nucleus, surrounding it completely. The rest of

the nucleus appears weekly and irregularly stained or not stained at all. In addition, Mitotic cells do not show staining of the chromosome region, ruling out a homogenous staining pattern. Lamin and dsDNA are among the antigens that might depict this pattern of staining.

Western Blotting

One representative supernatant for each staining pattern was picked for further analysis by Western blotting (Figure 3-4). Each supernatant tested showed different degrees of reactivity against whole cell fraction of Hep-2 cells transferred to a PVDF membrane. Samples 2E6, 5A9, and 5C1 reacted more favorable, while samples 5A10, 4F12, and 1G7 reacted very faintly or almost showed no reactivity at all. Samples 2E6 and 5A9 showed various bands within the range of 25 to 75 kDa that looked like promising representatives of critical autoantibodies. Sample 5C1 showed two bands between 50 and 75 kDa that suggested further evaluation as well. Samples 4F12 and 1G7 showed very weak reactivity, and sample 5A10 showed no reactivity at all, perhaps indicating that the blotting technique needed to be re-designed to meet special needs related to incubation conditions and dilution of the supernatants. Supernatants 4F12, 1G7, and 5A10 did not yield interesting blotting reactivity compatible with the results illustrated by the immunofluorescence staining.

Immunoprecipitation

Electrophoresis analysis of samples and controls showed different banding pattern on both immunoprecipitation assays (Figure 3-5 and 3-7). Differences were observed in number, size, and intensity of bands. However, similarities were also observable after in-depth comparison. Sample 2E6 showed interesting bands at approximately 100, 60, 45, and 20 kDa for antibodies exposed to cytoplasmic fractions of Hep-2 cells and 100, 60, 54, 52, 45, 30 and 20 kDa for antibodies exposed to nuclear fractions (Figure 3-5, lanes 1 & 2). Sample 1G7 showed interesting bands at 100, 60, 54, 52, 45, and 20 kDa for antibodies exposed to cytoplasmic and

nuclear fraction of Hep-2, however the intensity of the bands depicted in the nuclear fraction appeared to be less intense than their similar counterparts in the cytoplasmic fraction of the same sample, perhaps indicating differences in protein concentration among the two fractions (Figure 3-7, lanes 5 & 6). Analysis of the electrophoresis pattern of serum from C57BL/6.NOD-*Aec1Aec2* mouse showed generally less reactivity than monoclonal supernatants (Figure 3-6, lane 3 and Figure 3-7 lanes 3 & 4). Specifically, antibodies from sera of this mouse reacted with antigens that appeared to be at approximately 75, 54, 52, 45, and 30 kDa when exposed to nuclear fractions of Hep-2 cells (Figure 3-6, lane 3). In the second immunoprecipitation assay, the band at 75 kDa appeared exclusively in mouse serum samples exposed to both cytoplasmic and nuclear extract of Hep-2 cells (Figure 3-7, lanes 3 & 4), but not in supernatant samples (Figure 3-7, lanes 1, 2, 5 & 6). This is consistent with results from the first immunoprecipitation assay. Bands at 45 and 30 kDa appeared both in serum and supernatant samples; however the intensity of the bands was weaker in serum samples, again, perhaps due to less protein concentration in serum compared to supernatants. Likewise, in gel 2 (Figure 3-7) bands at 54 and 52 kDa were present in all samples exposed to both cytoplasmic and nuclear fractions, but the intensity is slightly higher in supernatant samples of both 2E6 and 1G7 than in serum samples. However, in gel 1 (Figure 3-5) bands at 52 and 54 kDa were visible only in hybridoma 2E6 and serum from mice exposed to nuclear cellular fractions (Figure 3-5, lanes 2 & 3). Bands at 20 kDa appeared strong and well defined in supernatant samples of both 2E6 and 1G7, but not in whole serum samples. Electrophoresis pattern of samples representing washes showed efficient clearance of non-specific proteins at every step of the process during both immunoprecipitation assays (Figure 3-5, lanes 4-9, and Figure 3-7, lanes 5-8). Bands numbered 1, 2, 3, 4, 5, 6 and 7 from gel 1(Figure 3-6), and 8, 9 and 10 from gel two (Figure 3-8) were manually extracted for

sequencing analysis at the ICBR Protein Core Facility. Band molecular weight predictions were as follows: 100 kDa (band 1), 60 kDa (band 2), 54 kDa (band 3), 52 kDa (band 4), 45 kDa (band 5), 30 kDa (band 6), 75 kDa (band 7), 54 kDa (band 8), 52 kDa (band 9) and 20 kDa (band 10).

Protein Band Identification Using Band Sequencing Analysis

Protein sequencing of the 10 bands (where bands 8 and 9 were combined) by MS identified 91 unique proteins ranging from 6 proteins per band (band #3) to 29 proteins per band (band #5) (data not shown). Obviously, some proteins, especially keratins, were common to several (but not all) band sequences. Although several ways of analyzing the data were considered, e.g., molecular weights, presence in multiple bands, known autoantigens, and so forth, none proved to provide a reasonable and logical means to identify SSA/Ro, SSB/La, and anti M3R autoantigens. Nevertheless, several other proteins were found that might have been expected based on the known nuclear autoantigens of human SS and mice SS-like disease (table 3-2). These included several histone and ribonuclear proteins, plus ribosomal proteins. Similarly, the structural protein units of keratin were also identified in both nuclear and cytoplasmic extracts by hybridoma supernatants, as well as whole sera from diseased C57BL/6.NOD-*Aec1Aec2* mice. These data, while not identifying precise autoantigens of known importance, establish a basis that should yield such identifications. Thus, the results provide strong support to this approach, even though any future approach will require modification.

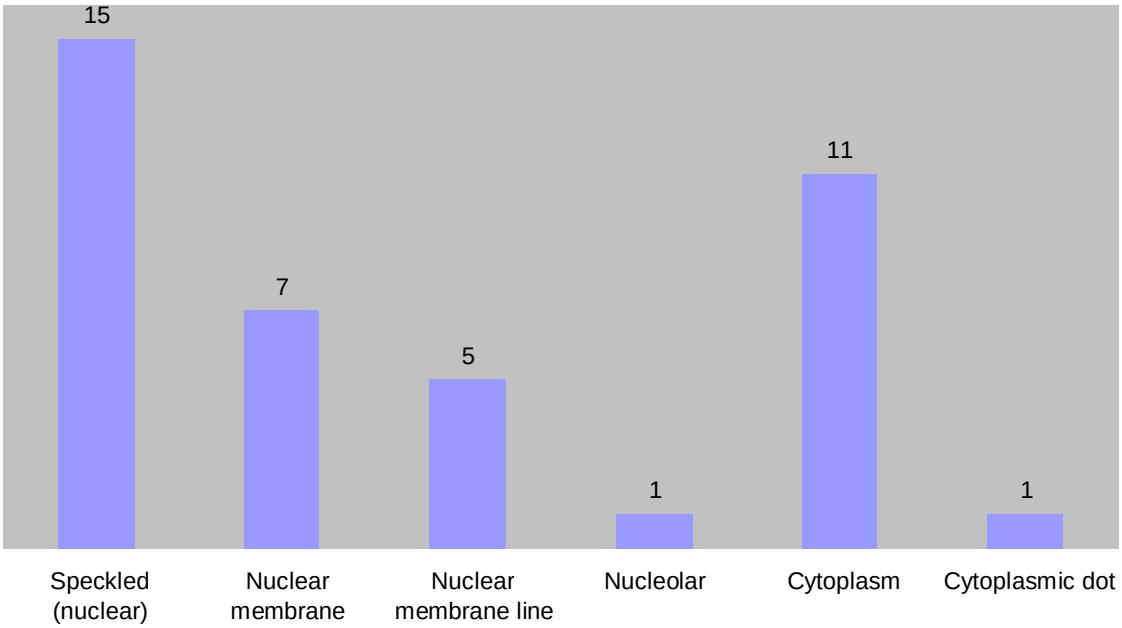

Figure 3-1. Absolute distribution of supernatants according to staining patterns

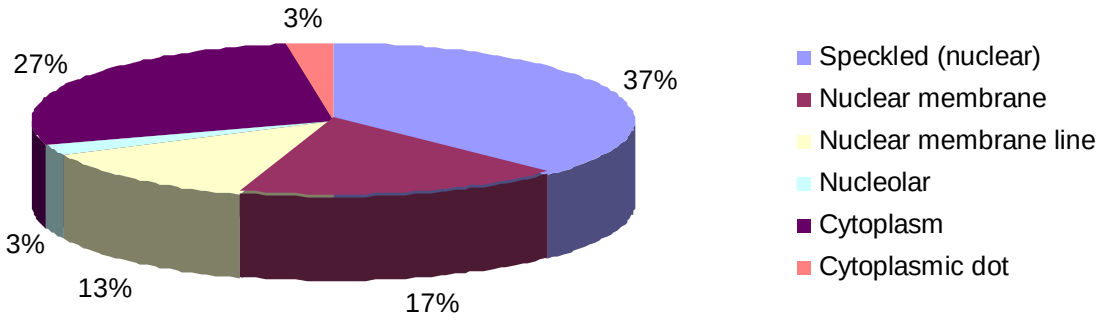

Figure 3-2. Relative distribution of supernatants according to staining patterns

Table 3-1. Staining pattern of antibody-secreting hybridomas by Indirect Immunofluorescence

Hybridoma	Staining pattern	Titer	Exposure Time
3B2	Speckled nuclear	1/50	2 seconds
4A4	Cytoplasmic/cytoskeletal	1:50	2 seconds
2E6	Speckled nuclear	1:100	2 seconds
3B2	Speckled nuclear	1:50	2 seconds
5D9	Nuclear membrane line	1:100	3 seconds
1G7	Nuclear membrane/rim	Undiluted	2 seconds
5F11	Cytoplasmic/cytoskeletal	1:100	2 seconds
2E2	Nuclear membrane/rim	1:50	2 seconds
5D4	Cytoplasmic/cytoskeletal	1:100	3 seconds
5A9	Nuclear membrane line	1:50	2 seconds
4A4	Cytoplasmic/cytoskeletal	Undiluted	2 seconds
1C4	Speckled nuclear	1:50	2 seconds
3C10	Cytoplasmic/cytoskeletal	1:50	3 seconds
4H7	Nuclear membrane line	1:100	2 seconds
5B4	Speckled nuclear	1:50	2 seconds
4E1	Speckled nuclear	1:50	2 seconds
2H10	Nuclear membrane/rim	1:50	2 seconds
5C1	Cytoplasmic dot	1:50	3 seconds
5H11	Speckled nuclear	1:50	2 seconds
3E2	Speckled nuclear	1:50	3 seconds
5E1	Speckled nuclear	1:50	3 seconds
4B1	Cytoplasmic/cytoskeletal	1:50	3 seconds
IF9	Cytoplasmic/cytoskeletal	Undiluted	2 seconds
5G10	Nuclear membrane line	1:50	2 seconds
5F8	Cytoplasmic/cytoskeletal	1:50	2 seconds
4A5	Speckled nuclear	1:50	2 seconds
5D6	Nuclear membrane/rim	1:50	2 seconds
4F12	Cytoplasmic/cytoskeletal	1:100	2 seconds
5A10	Nucleolar	1:50	2 seconds
1H9	Speckled nuclear	1:50	2 seconds
4C8	Cytoplasmic/cytoskeletal	1:50	2 seconds
5A5	Nuclear membrane/rim	1:100	2 seconds
5D5	Speckled nuclear	1:50	2 seconds
5D9	Speckled nuclear	1:50	2 seconds
4B10	Speckled nuclear	1:50	2 seconds
3H6	Nuclear membrane line	1:50	2 seconds
1H7	Nuclear membrane/rim	1:50	2 seconds
2A4	Cytoplasmic/cytoskeletal	1:50	2 seconds
2E11	Nuclear membrane/rim	1:50	2 seconds
2G1	Speckled nuclear	1:100	2 seconds

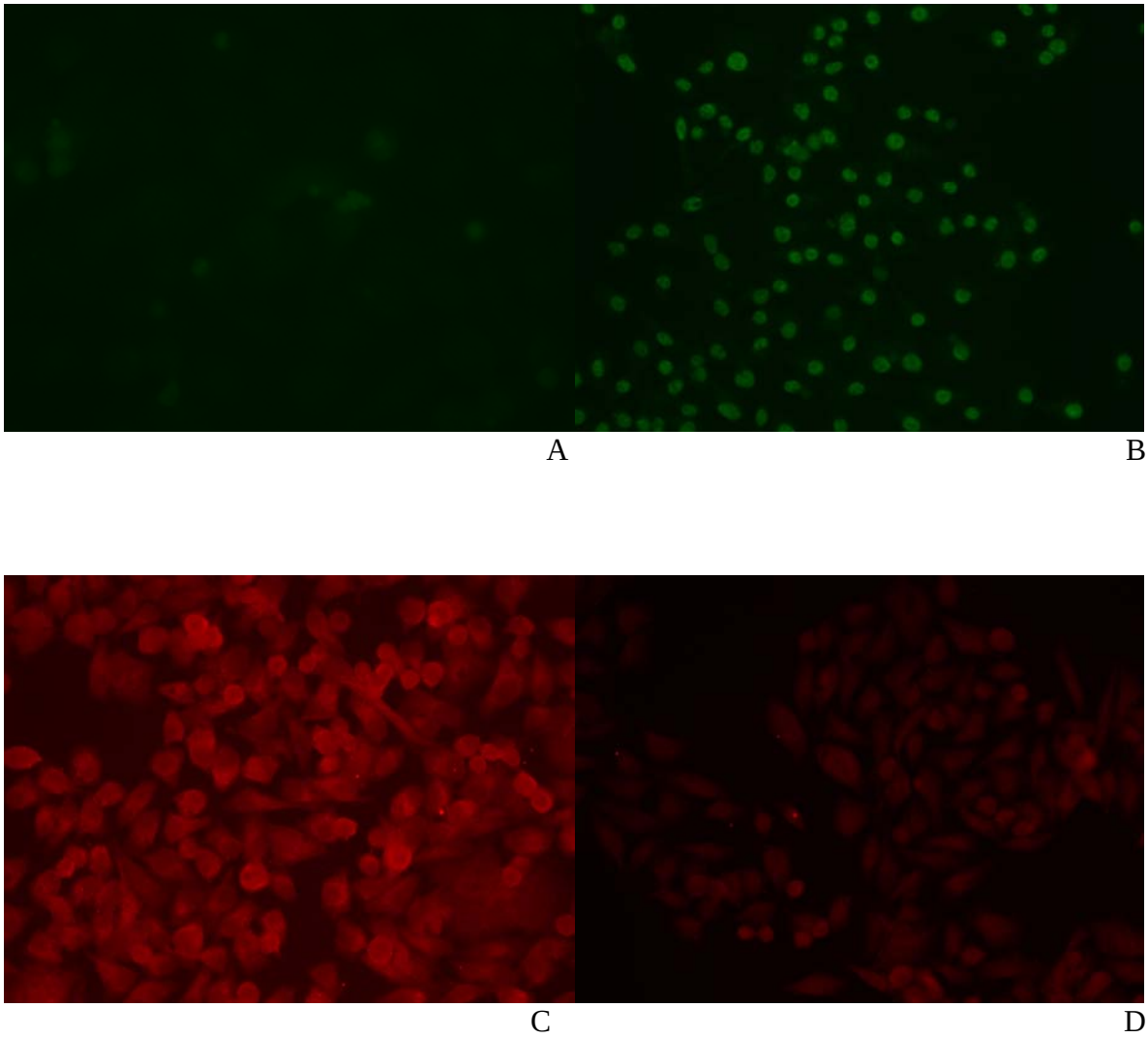

Figure 3-3. Indirect Immunofluorescence pattern of staining of Hep-2 cells. A) positive control; B) negative control; C) speckled pattern (clone 2E6); D) nuclear membrane line pattern (clone 5A9); E) cytoplasmic dot pattern (clone 5C1); F) nucleolar pattern (clone 5A10); G) cytoplasmic staining pattern (clone 4F12); H) nuclear membrane (rim) pattern (clone 1G7). Positive control consisted of human serum with antibody specific to nuclear antigens (Sigma Diagnostics, St. Louis, MO, Cat. # 2022). All pictures taken at 100x magnification

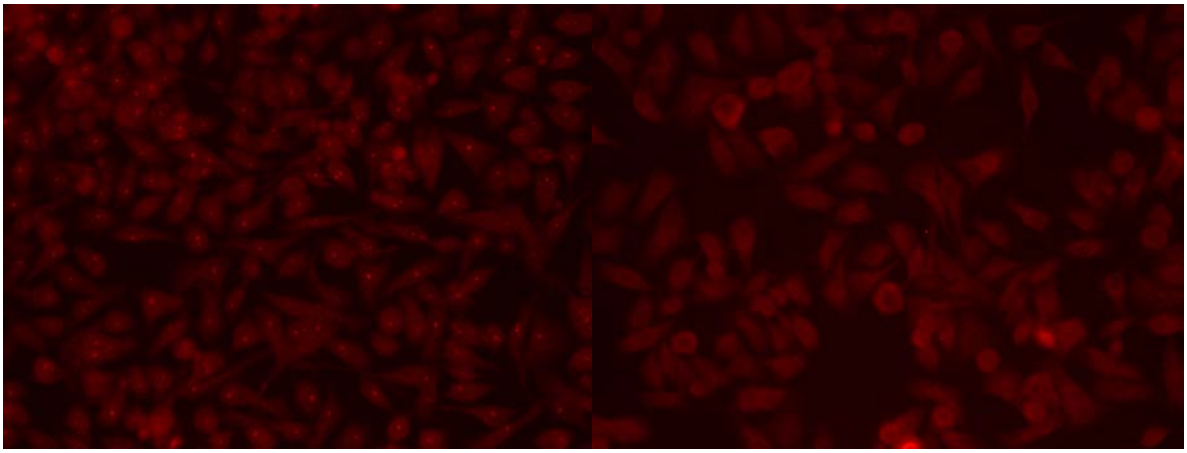

E F

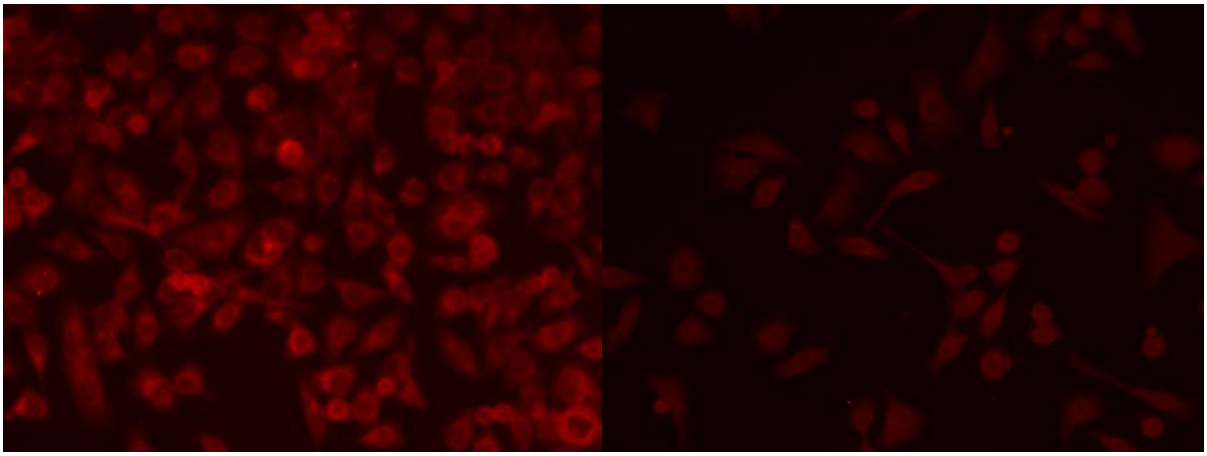

G H

Figure 3-3. Continued

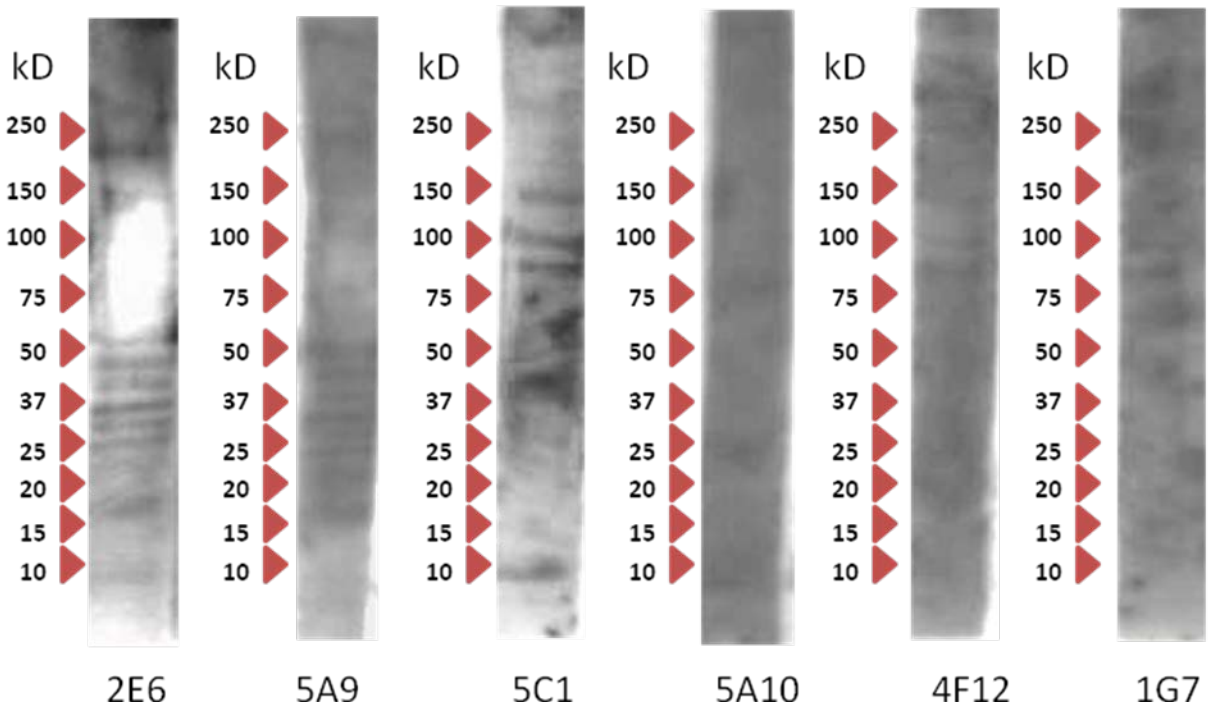

Figure 3-4. Western Blot

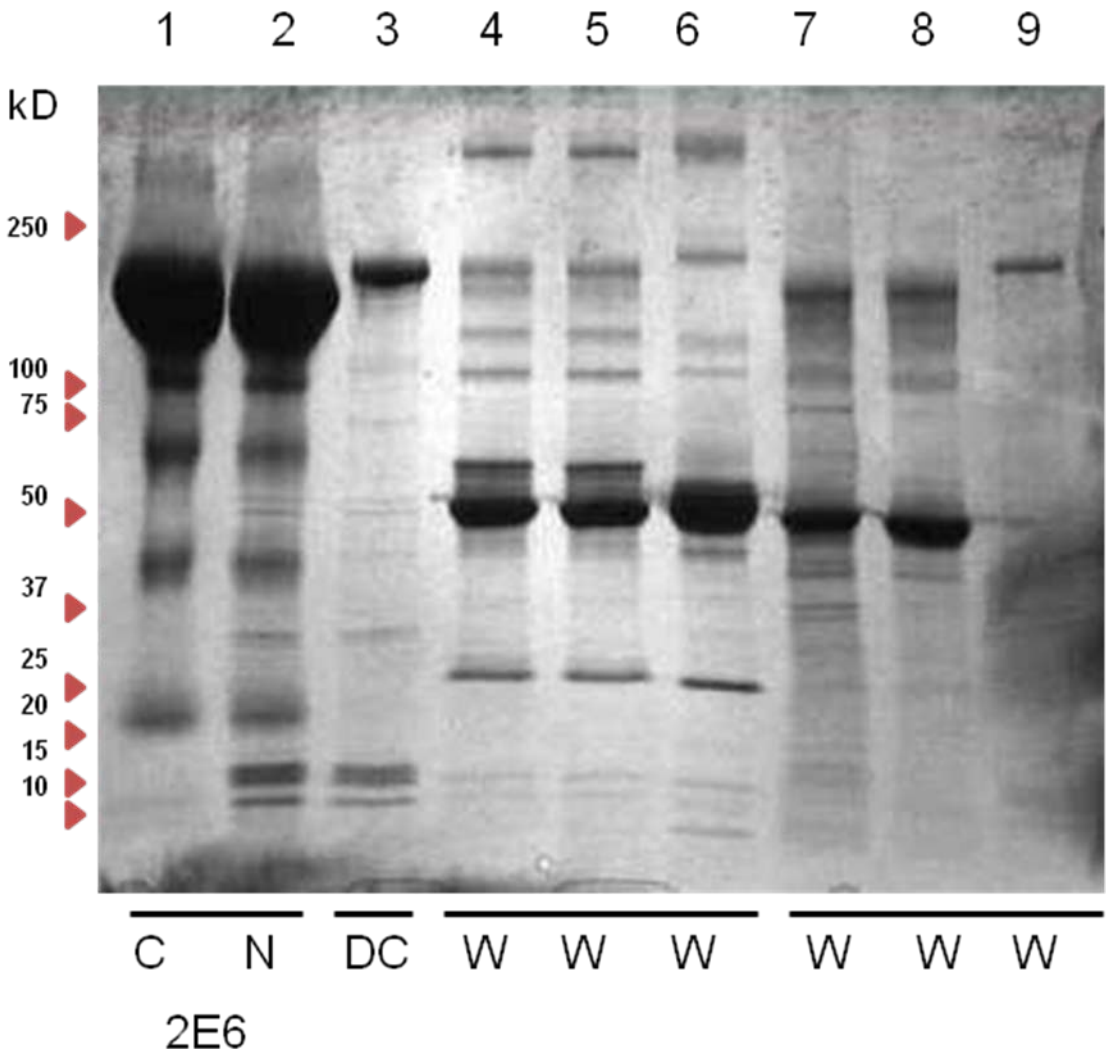

Figure 3-5. Immunoprecipitation: gel 1

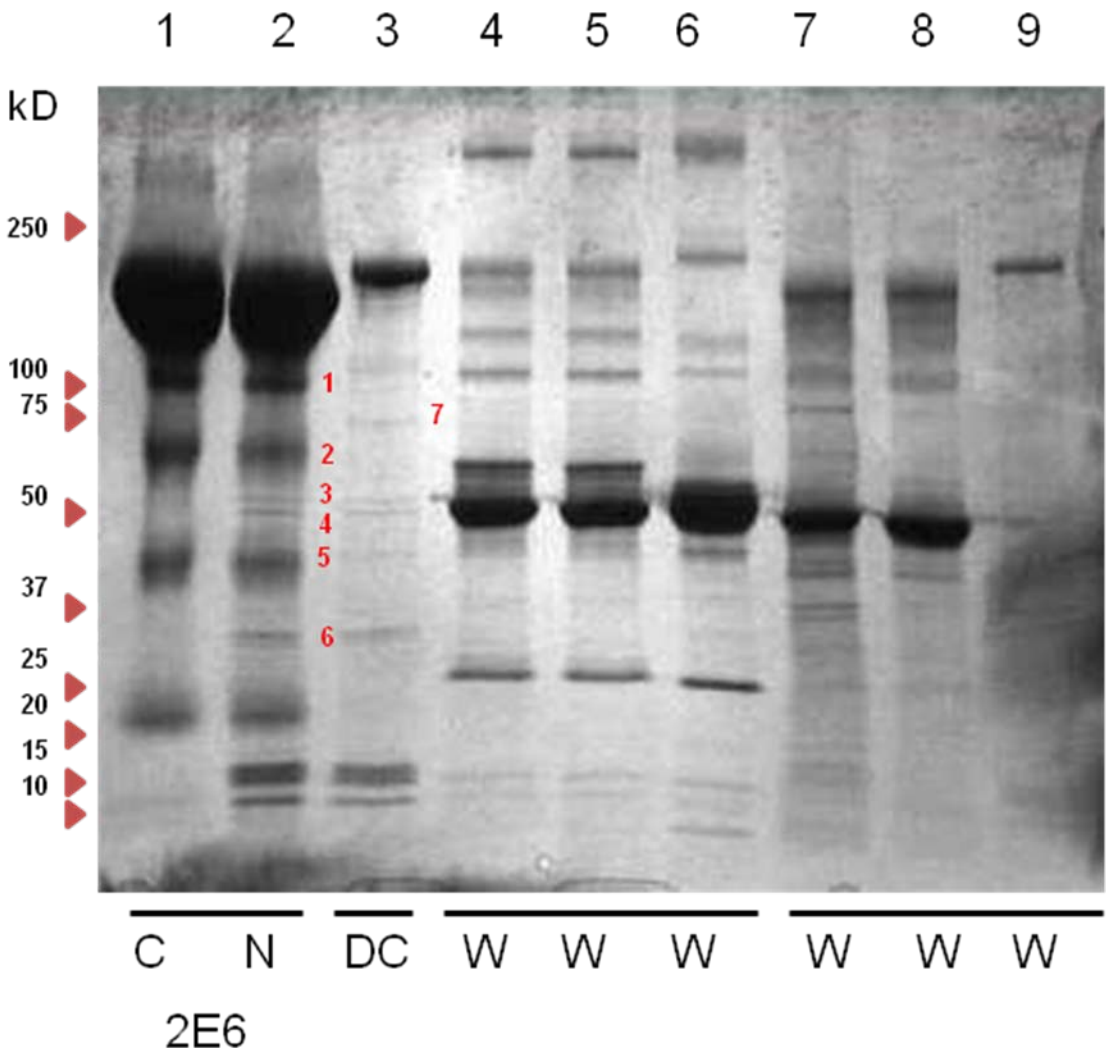

Figure 3-6. Immunoprecipitation: gel 1 with bands picked for analysis

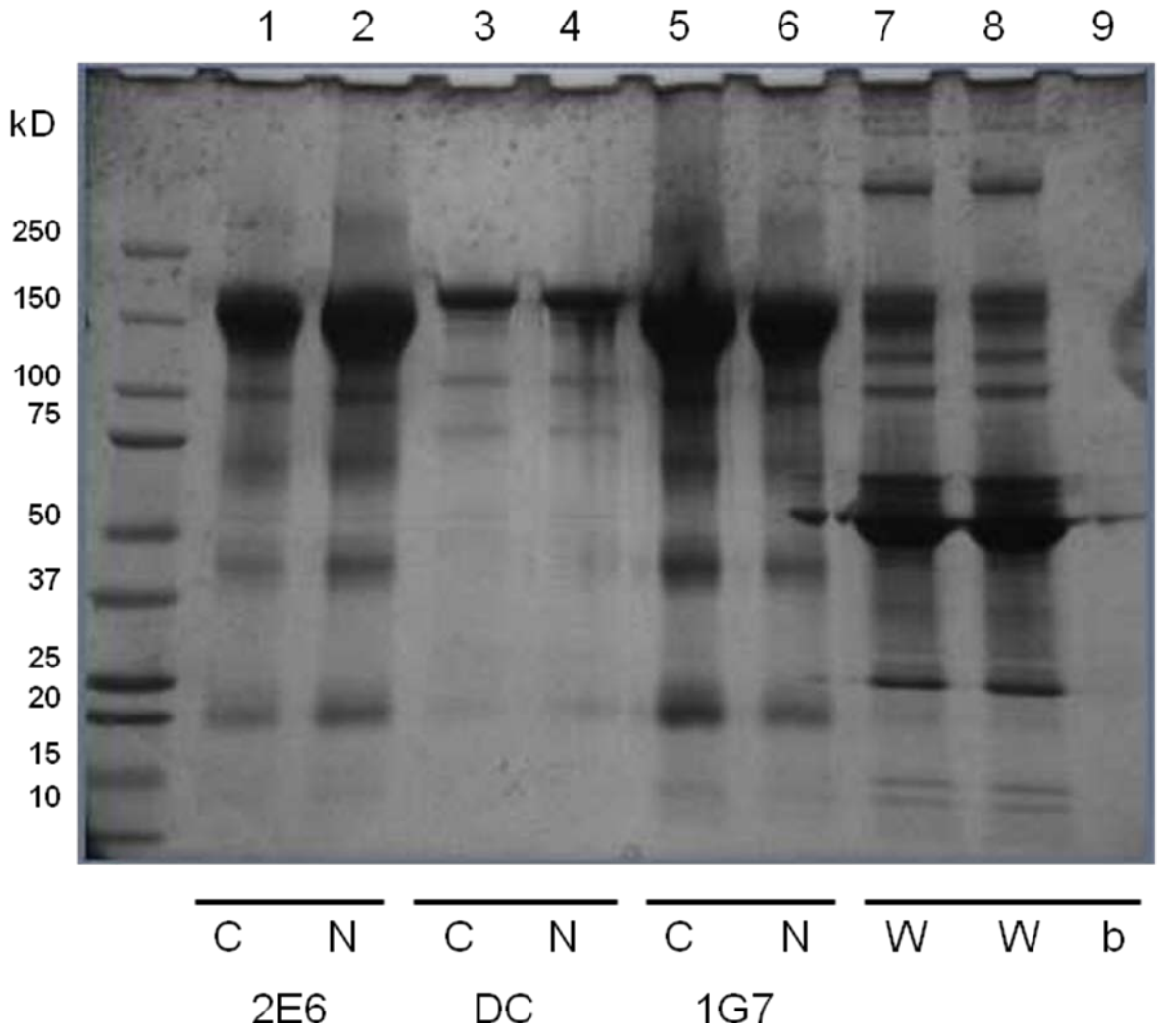

Figure 3-7. Immunoprecipitation: gel 2

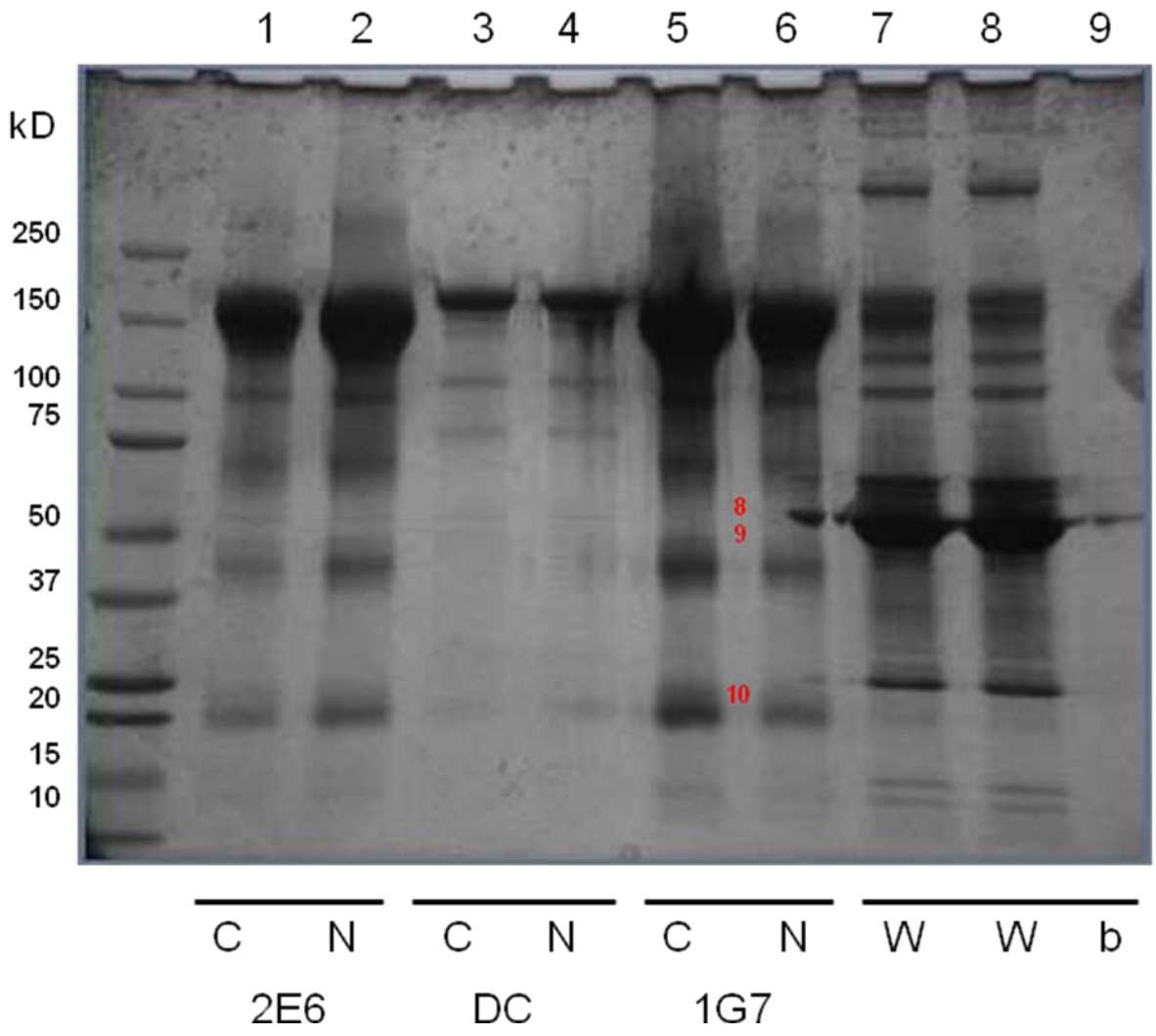

Figure 3-8. Immunoprecipitation: gel 2 with bands picked for analysis

Table 3-2. Proteins of putative importance found in the gels using mass spectrometry

Gel		1							2		
Band		1	2	3	4	5	6	7	8	9	10
Protein											
kD	Name										
56	Atp5b	X									
NR	Pmp2	X									
65	Lmna		X								
69	Ddx5		X								
78	Hnrpm		X								
61	Hp1bp3		X								
54	Vimentin			X					X	X	
63	Prosapip1				X	X			X	X	
207	Nes				X			X			
116	Srebf1				X						
84	Zfp184				X						
42	Actb					X					
69	Rngtt					X					X
42	Rbmx					X					
35	Ebna1bp2					X					
43	Ilf2					X					
51	Eef1a1					X					
46	Rpl3					X					
84	Ctcf					X					
21	Hist1h1c						X				
27	Sfrs7						X				
27	Rps3						X				
23	Hist1h1b						X				
32	Rps2						X				
34	Cdc2a						X				
20	H1fx						X				
30	Rps3a						X				
25	Sfrs2						X				
30	Rps4x						X				
72	Cabc1								X	X	
65	Mettl3								X	X	
158	Ssh2										X

CHAPTER 4
DISCUSSION

The overall goal of this project was to initiate a characterization of monoclonal antibodies (mAbs) secreted by a set of hybridomas generated from fusions involving B lymphocytes present in the draining cervical lymph nodes of C57BL/6.NOD-Aec1Aec2 mice diagnosed with early-stage Sjögren's syndrome-like disease. The specific issue in question was whether or not was possible to identify specific autoantigens being recognized during the development and/or onset of autoimmunity involving the salivary glands. The approach entailed three steps: 1) define the general staining pattern of each monoclonal antibodies-containing clone, 2) determine by western blot and immunoprecipitation if mAbs contained in the clones bind to unique proteins, and 3) carry out a preliminary analysis of proteins isolated by IP using GC-mass spec sequencing.

Indirect immunohistochemistry and western blot analysis are the methods of choice for general initial characterization of supernatants' content. Immunoprecipitation and band sequencing analysis have the potential to provide more specific identification of supernatants' content. Indirect immunohistochemistry was used to detect patterns of staining of antinuclear autoantibodies, thus, providing initial clues regarding the localization of target antigens. Indirect immunohistochemistry is a very common method to detect proteins in cells and/or tissues. A cell disruption and fixation method was required to allow for localization of cytoplasmic and nuclear antigens by immobilization of the proteins. Using this technique, it was shown that the spectrum of autoantibody reaction to cellular antigens is wider than anticipated. Most likely, the pathological and clinical relevance of all putative autoantibodies secreted by hybridomas is not the same. However, since most auto-antigens are potentially involved in important cellular functions, any single one that could be found and characterized in the supernatants represents a

new opportunity to attain a better understanding of the complicated pathogenesis of Sjögren's syndrome-like disease in the mouse model.

Ro/SSA and La/SSB are considered clinical markers of the disease in human. Staining patterns of Hep-2 cells obtained in this study do not exactly recapitulate the classical speckled patterns describe before for these auto-antibodies. There might be some explanations for this; being the most notorious the fact that anti-SS/A reacts with an epitope located in the 60 kD protein which is exclusive of humans (Cook L., 1998). Additional autoantigens identified in autoimmune diseases are ribonucleoproteins targeted by autoantibodies such as anti-sm or anti-RNP, topoisomerase-I proteins targeted by anti-Scl-70 auto-antibodies, and enzymes associated with tRNA metabolism targeted by anti-Jo-1 autoantibodies. Staining patterns obtained might be associated with these auto-antigens but further analysis was required.

By using mAbs-containing supernatants on Western blots of whole crude lysate of Hep-2 cells it was possible to characterize more specific reactivity patterns according to the molecular weight of the bands depicted on the blot. Reactivity differed from relatively high (supernatants 2E6, 5A9, and 5C1) to low or non-existent (supernatants 5A10, 4F12, and 1G7). Such a variable reaction among the samples might be explained by different degrees of binding specificity of the auto-antibodies, or by assay-related conditions that failed to meet minimum requirements for antigen-antibody epitope recognition. However, the results were promising for those samples that showed some degree of reactivity and they led to new clues toward antigen identification. Both cytoplasmic and nuclear extracts from Hep-2 cells were proven to be an adequate source of antigen for immunoprecipitation protocols when using monoclonal supernatant from mouse as an antibody. An advantage of the immunoprecipitation is that isolates likely autoantibodies away

from non-relevant proteins. Non-relevant proteins were perhaps the cause of high background and low band definition in some of the samples tested (supernatants 5A10, 4F12, and 1G7). The high intensity of the bands of samples' lanes is an indication of high concentration and/or abundance of the antigen in the cellular sub-fractions. The intensity was different among bands but was stronger that the banding pattern from mouse serum. This finding is indicative of higher concentration of antigen in tissues rather than in serum, and presence of autoantibody-secreting B-cell close by or within the target organs.

Supernatants gave a fairly clean immunoprecipitation assay compared with the Western blot results. This finding is interesting; it might indicate not only that the antigen is abundant in the cells but also that the mAbs contained in the supernatant have high affinity for their antigens despite of the fact that usually their titer is lower compared to those of ascitis fluids. A clean assay with well defined bands was crucial for band prediction and selection for further and more specific analysis using GC-mass spec sequencing.

GC-mass spec sequencing identified 91 diverse proteins, but whether or not these represent autoantigens remains questionable and will require further separation and characterization. Sequencing whole bands based on Coomassie Blue staining of one-dimensional gels is apt to provide multiple proteins. Two interesting observations are: 1) many of the proteins identified in this manner are not of the MW_R expected, suggesting considerable breakdown, digestion and/or alternative splicing, and 2) several of the identified proteins fall into categories considered to be possible candidate autoantigens, for example, histone, ribonuclear and ribosome-associated proteins. Additional proteins of interest include vimentin, nestin and keratin, three molecules suggested in the literature to be autoantigens under specific conditions. One unexpected result, but one that is clearly derived from the gel patterns, is the multiple banding that each supernatant

exhibits on immunohistochemical staining and Western blotting. This suggests that the hybridomas contain more than one monoclonal antibody (mAb) and that each hybridoma requires cloning prior to further analysis.

REFERENCES

Bennett J (2008). The role of T lymphocytes in rheumatoid arthritis and other autoimmune diseases. *Arthritis Rheum* 58(2 Suppl):S53-7.

Boire G, Gendron M, Monast N, Bastin B, Ménard H (1995). Purification of antigenically intact Ro ribonucleoproteins; biochemical and immunological evidence that the 52-kD protein is not a Ro protein. *Clin Exp Immunol* 100(3):489-98.

Brayer J, Cha S, Nagashima H, Yasunari U, Lindberg A, Diggs S, Martinez J, Goa J, Humphreys-Beher M, Peck A (2000). IL-4-dependent effector phase in autoimmune exocrinopathy as defined by the NOD.IL-4-gene knockout mouse model of Sjögren's syndrome. *Scand J Immunol* 54(1-2):133-40.

Brayer J, Lowry J, Cha S, Robinson C, Yamachika S, Peck A, Humphreys-Beher M (2000). Alleles from chromosomes 1 and 3 of NOD mice combine to influence Sjögren's syndrome-like autoimmune exocrinopathy. *J Rheumatol* 27(8):1896-904.

Carrillo J, Puertas M, Alba A, Ampudia R, Pastor X, Planas R, Riutort N, Alonso N, Pujol-Borrell R, Santamaria P, Vives-Pi M, Verdaguer J (2005). Islet-infiltrating B-cells in nonobese diabetic mice predominantly target nervous system elements. *Diabetes* 54(1):69-77.

Cavill D, Waterman S, Gordon T (2003). Antiidiotypic antibodies neutralize autoantibodies that inhibit cholinergic neurotransmission. *Arthritis Rheum* 48(12):3597-602.

Cha S, Nagashima H, Brown V, Peck A, Humphreys-Beher M (2002). Two NOD Idd-associated intervals contribute synergistically to the development of autoimmune exocrinopathy (Sjögren's syndrome) on a healthy murine background. *Arthritis Rheum* 46(5):1390-8.

Cha S, Singson E, Cornelius J, Yagna J, Knot H, Peck A (2006). Muscarinic acetylcholine type-3 receptor desensitization due to chronic exposure to Sjögren's syndrome-associated autoantibodies. *J Rheumatol* 33(2):296-306.

Cook L. New Methods for Detection of Anti-nuclear Antibodies (1998). *Clinical Immunology and Immunopathology: Academic Press*. p. 211-20.

de Wilde P, Kater L, Bodeutsch C, van den Hoogen F, van de Putte L, van Venrooij W (1996). Aberrant expression pattern of the SS-B/La antigen in the labial salivary glands of patients with Sjögren's syndrome. *Arthritis Rheum* 39(5):783-91.

Dupond J, Gil H, Bouhaddi M, Magy N, Berthier S, Regnard J (1999). Acute dysautonomia secondary to autoimmune diseases: efficacy of intravenous immunoglobulin and correlation with a stimulation of plasma norepinephrine levels. *Clin Exp Rheumatol* 17(6):733-6.

Encinas J, Wicker L, Peterson L, Mukasa A, Teuscher C, Sobel R, Weiner H, Seidman C, Seidman J, Kuchroo V (1999). QTL influencing autoimmune diabetes and encephalomyelitis map to a 0.15-cM region containing Il2. *Nat Genet* 21(2):158-60.

Fei H, Kang H, Scharf S, Erlich H, Peebles C, Fox R (1991). Specific HLA-DQA and HLA-DRB1 alleles confer susceptibility to Sjögren's syndrome and autoantibody production. *J Clin Lab Anal* 5(6):382-91.

Fox R (2005). Sjögren's syndrome. *Lancet* 366(9482):321-31.

Gao J, Cha S, Jonsson R, Opalko J, Peck A (2004). Detection of anti-type 3 muscarinic acetylcholine receptor autoantibodies in the sera of Sjögren's syndrome patients by use of a transfected cell line assay. *Arthritis Rheum* 50(8):2615-21.

Gao J, Killedar S, Cornelius J, Nguyen C, Cha S, Peck A (2006). Sjögren's syndrome in the NOD mouse model is an interleukin-4 time-dependent, antibody isotype-specific autoimmune disease. *J Autoimmun* 26(2):90-103.

Golan T, Elkon K, Gharavi A, Krueger J (1992). Enhanced membrane binding of autoantibodies to cultured keratinocytes of systemic lupus erythematosus patients after ultraviolet B/ultraviolet A irradiation. *J Clin Invest* 90(3):1067-76.

Gottlieb E, Steitz J (1989). Function of the mammalian La protein: evidence for its action in transcription termination by RNA polymerase III. *EMBO J* 8(3):851-61.

Hill N, Lyons P, Armitage N, Todd J, Wicker L, Peterson L (2000). NOD Idd5 locus controls insulitis and diabetes and overlaps the orthologous CTLA4/IDDM12 and NRAMP1 loci in humans. *Diabetes* 49(10):1744-7.

Kaufmann T, Schinzel A, Borner C (2004). Bcl-w(edding) with mitochondria. *Trends Cell Biol* 14(1):8-12.

Luhder F, Chambers C, Allison J, Benoist C, Mathis D (2000). Pinpointing when T cell costimulatory receptor CTLA-4 must be engaged to dampen diabetogenic T cells. *Proc Natl Acad Sci U S A* 97(22):12204-9.

Lühder F, Höglund P, Allison J, Benoist C, Mathis D (1998). Cytotoxic T lymphocyte-associated antigen 4 (CTLA-4) regulates the unfolding of autoimmune diabetes. *J Exp Med* 187(3):427-32.

Lundholm M, Motta V, Löfgren-Burström A, Duarte N, Bergman M, Mayans S, Holmberg D (2006). Defective induction of CTLA-4 in the NOD mouse is controlled by the NOD allele of Idd3/IL-2 and a novel locus (Ctex) telomeric on chromosome 1. *Diabetes* 55(2):538-44.

Mavragani C, Tzioufas A, Moutsopoulos H (2000). Sjögren's syndrome: autoantibodies to cellular antigens. Clinical and molecular aspects. *Int Arch Allergy Immunol* 123(1):46-57.

Nguyen C, Cha S, Peck A (2007). Sjögren's syndrome (SjS)-like disease of mice: the importance of B lymphocytes and autoantibodies. *Front Biosci* 12:1767-89.

Nguyen C, Cornelius J, Cooper L, Neff J, Tao J, Lee B, Peck A (2008). Identification of possible candidate genes regulating Sjögren's syndrome-associated autoimmunity: a potential role for TNFSF4 in autoimmune exocrinopathy. *Arthritis Res Ther* 10(6):R137.

Nguyen C, Kim H, Cornelius J, Peck A (2007). Development of Sjogren's syndrome in nonobese diabetic-derived autoimmune-prone C57BL/6.NOD-Aec1Aec2 mice is dependent on complement component-3. *J Immunol* 179(4):2318-29.

Nguyen C, Cornelius J, Singson E, Killedar S, Cha S, Peck A (2006). Role of complement and B lymphocytes in Sjögren's syndrome-like autoimmune exocrinopathy of NOD.B10-H2b mice. *Mol Immunol* 43(9):1332-9.

Nguyen C, Singson E, Kim J, Cornelius J, Attia R, Doyle M, Bulosan M, Cha S, Peck A (2006). Sjögren's syndrome-like disease of C57BL/6.NOD-Aec1 Aec2 mice: gender differences in keratoconjunctivitis sicca defined by a cross-over in the chromosome 3 Aec1 locus. *Scand J Immunol* 64(3):295-307.

Petros A, Olejniczak E, Fesik S (2004). Structural biology of the Bcl-2 family of proteins. *Biochim Biophys Acta* 1644(2-3):83-94.

Robinson C, Brayer J, Yamachika S, Esch T, Peck A, Stewart C, Peen E, Jonsson R, Humphreys-Beher M (1998). Transfer of human serum IgG to nonobese diabetic Igmu null mice reveals a role for autoantibodies in the loss of secretory function of exocrine tissues in Sjögren's syndrome. *Proc Natl Acad Sci* U S A 95(13):7538-43.

Robinson C, Yamachika S, Bounous D, Brayer J, Jonsson R, Holmdahl R, Peck A, Humphreys-Beher M (1998). A novel NOD-derived murine model of primary Sjögren's syndrome. *Arthritis Rheum* 41(1):150-6.

Sundvall M, Jirholt J, Yang H, Jansson L, Engström A, Pettersson U, Holmdahl R (1995). Identification of murine loci associated with susceptibility to chronic experimental autoimmune encephalomyelitis. *Nat Genet1* 10(3):313-7.

Tengnér P, Halse A, Haga H, Jonsson R, Wahren-Herlenius M (1998). Detection of anti-Ro/SSA and anti-La/SSB autoantibody-producing cells in salivary glands from patients with Sjögren's syndrome. *Arthritis Rheum* 41(12):2238-48.

Varga J (2008). Systemic sclerosis: an update. *Bull NYU Hosp Jt Dis* 66(3):198-202.

Vitali C, Bombardieri S, Jonsson R, Moutsopoulos H, Alexander E, Carsons S, Daniels T, Fox P, Fox R, Kassan S, Pillemer S, Talal N, Weisman M (2002). Classification criteria for Sjögren's syndrome: a revised version of the European criteria proposed by the American-European Consensus Group. *Ann Rheum Dis* 61(6):554-8.

Waterman S, Gordon T, Rischmueller M (2000). Inhibitory effects of muscarinic receptor autoantibodies on parasympathetic neurotransmission in Sjögren's syndrome. *Arthritis Rheum* 43(7):1647-54.

Yamamoto H, Sims N, Macauley S, Nguyen K, Nakagawa Y, Humphreys-Beher M (1996). Alterations in the secretory response of non-obese diabetic (NOD) mice to muscarinic receptor stimulation. *Clin Immunol Immunopathol* 78(3):245-55.

Yannopoulos D, Roncin S, Lamour A, Pennec Y, Moutsopoulos H, Youinou P (1992). Conjunctival epithelial cells from patients with Sjögren's syndrome inappropriately express major histocompatibility complex molecules, La(SSB) antigen, and heat-shock proteins. *J Clin Immunol* 12(4):259-65.

BIOGRAPHICAL SKETCH

The author was born in Maracaibo, Venezuela and raised in Maracaibo and Sant Cougat del Vallès, Spain. Back in Venezuela, he attended Colegio Claret, where he completed his middle and high school education. He continued his academic endeavors by completing a M.D. degree at Universidad del Zulia in his home city. For four years he worked as a physician in rural areas of the east and west coast of Venezuela. Then he moved to the United States to pursue his Master of Public Health and Master of Science degrees at the University of Florida. He aspires to follow studies leading to a Ph.D. degree.